Available online at www.sciencedirect.com
ScienceDirect
Journal of Power Sources 163 (2006) 584–590
JOURNAL OF POWER SOURCES
www.elsevier.com/locate/jpowsour

The novel state of charge estimation method for lithium battery using sliding mode observer

Il-Song Kim *

LG Chem Research Park, 104-1, Moonji-Dong, Yuseong-Gu, Daejeon 305-380, Republic of Korea

Received 6 June 2006; received in revised form 16 August 2006; accepted 14 September 2006
Available online 27 October 2006

Abstract

In this paper, a new state of charge estimation method for lithium battery has been presented. Contrary to the conventional methods which use complicated battery modeling, a simple resistor–capacitor battery model was used in order to reduce calculation time and system resource. Modeling errors caused by the simple model are compensated by the sliding mode observer. The structure of the proposed system is simple, but it shows robust control property against modeling errors and uncertainties. The state equation for battery model and the systematic design approach for sliding mode observer also have been presented. The convergence of proposed observer has been proved by the Lyapunov inequality equation and the performance of system has been verified by the sequence of urban dynamometer driving schedule test. The test results show the proposed observer system has robust tracking performance with reduced calculation time under the real driving environments.

Keywords: State of charge estimation; Sliding mode observer; SOC; Lithium battery modeling

1. Introduction

Lithium-ion or lithium-polymer batteries are widely used in the mobile equipment, electric vehicle, space and aircraft power systems for their high energy density, high galvanic potential and long lifetimes compared to the lead-acid battery or nickel-metal hydride batteries. Due to the complex chemical and physical process of the battery, the behavior of battery is hard to predict compared with that of electric and mechanic devices. There are several parameters associated with battery behavior. The key parameter will be the state of charge (SOC) of the battery. The SOC corresponds to the stored charge available to do work relative to that which is available after the battery has been fully charged. SOC can be viewed as a thermodynamic quantity, enabling one to assess the potential energy of the system. Since the battery charge/discharge current control is based on the SOC information, the correct indication of SOC are of considerable importance such as hybrid electric vehicle (HEV) application. Since there is no sensor available to measure SOC, it should be estimated from physical measurements by some mathematical algorithm.

There have been many attempts to estimate the SOC of batteries. The most common methods are the charge counting and Kalman filter approach. Charge counting or current integration is the most commonly used technique, requiring dynamic measurement of the battery charge–discharge current, the time integral of which is considered to provide a direct indication of SOC [1]. However, the charge counting is an open loop SOC estimator and thus the errors in the current detector are accumulated by the estimator. The error is due to noise, resolution, and rounding are cumulative and large SOC errors can result. A reset or recalibration action is, therefore, required at regular intervals—in all electric vehicles. This may be carried out during a full charge or conditioning discharge, but is less appropriate for standard HEV operation where full SOC is rarely achieved.

Cell-impedance measurements have also been reported as a useful technique for resetting or adjusting SOC estimates from integration based methods. However, from results of various studies undertaken to identify the impedance variation of battery, with SOC, contradictory views to their usefulness in practical systems currently remain unresolved [2].

* Tel.: +82 42 870 6345; fax: +82 42 870 6052.
E-mail address: iskim@powerlab.kaist.ac.kr.

0378-7753/$ – see front matter © 2006 Elsevier B.V. All rights reserved.
doi:10.1016/j.jpowsour.2006.09.006

Nomenclature

A, B, Γ, ξ	system parameters
C_n	nominal capacity of the cell (Ah)
C_p	polarization capacitance (F)
e	error states
Δf_1, Δf_2, Δf_3	modeling errors and uncertainties
H	gain matrix
P, Q, P_f, Q_f, R	positive definite gain matrix
R_p	diffusion resistor (Ω)
R_t	ohmic resistance (Ω)
$V_{oc}(Z)$	open-circuit voltage as a function of SOC Z
V_p	polarization voltage (V)
$\hat{V}_p$	estimate of the polarization voltage (V)
V_t	cell terminal voltage (V)
$\hat{V}_t$	estimate of the cell terminal voltage (V)
x	system states
y	output state
Z	state of charge
$\hat{Z}$	estimate of the state of charge

Greek letter

ρ	switching gain

The Kalman filter methods are well known technology for dynamic system state estimation such as target tracking, navigation and battery field [3,4]. It provides a recursive solution to optimal linear filtering, for both state observation and prediction problems. The unique advantage of the Kalman filter is that it optimally estimates states affected by broadband noise contained within the system bandwidth. The drawbacks of Kalman filter are difficulties of feedback gain selection. If the gain is not properly selected, the estimated states will diverge. Also Kalman filter have some limitations for a real implementation such as perfect modeling of the plant and Gaussian distribution of the external noise. If these constraints are not satisfied, the performance of the Kalman filter will be degraded and thus cannot be used in the real applications.

Other reported methods for estimating the SOC have been based on artificial neural networks and fuzzy logic principles [5,6]. Since these techniques incur large computation overhead on the battery management controller, it can be a problem for online implementation. If high performance digital signal processing (DSP) chips are used as controller, neural networks, in particular, can reduce the calculation loads for large number of empirically derived parameters required by other methods.

In this paper, the new sliding mode observer design method has been proposed for the battery SOC estimation. The proposed sliding mode observer can overcome the above mentioned drawbacks by using sliding mode techniques. Sliding mode control was first introduced by Utkin [7]. It is a technique robust in the presence of parameter uncertainties and disturbances. It entails the construction of an equilibrium manifold and a control, designed to drive the system state to the sliding manifold and maintain it on the equilibrium manifold. The equilibrium manifold is constructed so that the system restricted to the manifold has a desired behavior. As the sliding mode controller has been known to have the robustness under the presence of parameter variations and disturbance, the sliding mode observers are also known to have similar robustness properties [8–10]. The main characteristic of the sliding mode observer is that it has robust tracking performance under modeling uncertainties environments and simple control structure.

2. Battery modeling

There have been many attempts to develop battery modeling. The most common methods are electro-chemistry model and electro-circuit model. While detailed chemistry-based models have been built to investigate the internal dynamics of the battery, these models are generally not suitable for electrical system design approach [11]. On the other hand, circuit-based models have been built by the electric circuit parameters such as capacitor, resistor, voltage source and so on [12]. It is commonly used method for battery controller, because it is possible to express as mathematical formulas. It has been known that perfect battery modeling is hard to achieve for every operating conditions using the electro-circuit model. Therefore, many complicated electrical modeling methods have been developed to reduce modeling errors. However, these methods increase the calculation time, system complexity, resources and they can be a cause of instability.

A simple resistor–capacitor model is employed to the lithium battery modeling in this paper. All of the modeling errors, uncertainties, and time varying elements are considered as external disturbance at all. The merit of this model is simple, little computational time, and the modeling errors are compensated in the robust sliding mode observer.

A resistor–capacitor electrical model of lithium-polymer battery consists of non-linear voltage source $V_{oc}(Z)$ as a function of SOC Z, a capacitance C_p to model chemical diffusion of the electrolyte within the battery, a diffusion resistance R_p as a function of current I, an ohmic resistance R_t and terminal voltage V_t. The resistor–capacitor electrical model including uncertainties is shown in Fig. 1. The terminal voltage is given as

$$V_t = V_{oc}(Z) + IR_t + V_p \tag{1}$$

The time derivative for SOC Z can be expressed as follows:

$$\dot{Z} = \frac{I}{C_n} = \frac{1}{R_t C_n}(V_t - V_{oc}(Z) - V_p) \tag{2}$$

where I is the instantaneous current and C_n is the nominal capacity of the cell. The polarization voltage due to the current is shown as

$$\dot{V}_p = -\frac{1}{R_p C_p} V_p + \frac{I}{C_p} \tag{3}$$

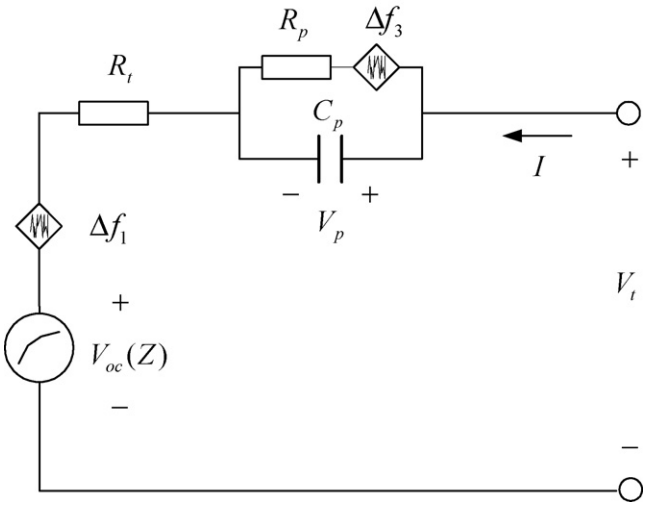

Fig. 1. The resistor–capacitor electrical modeling of lithium battery.

The time derivative of V_t is obtained by assuming $dI/dt = 0$, and the complete state equation is given as

$$\begin{aligned}
\dot{V}_t &= V_{\mathrm{oc}}(\dot{Z}) + \dot{V}_{\mathrm{p}} = \frac{I}{C_{\mathrm{n}}} - \frac{1}{R_{\mathrm{p}}C_{\mathrm{p}}}V_{\mathrm{p}} + \frac{I}{C_{\mathrm{p}}} \\
&= -\frac{1}{R_{\mathrm{p}}C_{\mathrm{p}}}V_t + \frac{1}{R_{\mathrm{p}}C_{\mathrm{p}}}V_{\mathrm{oc}}(Z) + \left(\frac{1}{C_{\mathrm{n}}} + \frac{1}{C_{\mathrm{p}}} + \frac{R_t}{R_{\mathrm{p}}C_{\mathrm{p}}}\right) I \\
&= -a_1 V_t + a_1 V_{\mathrm{oc}}(Z) + b_1 I, \\
\dot{Z} &= a_2 V_t - a_2 V_{\mathrm{oc}}(Z) - a_2 V_{\mathrm{p}}, \qquad \dot{V}_{\mathrm{p}} = -a_1 V_{\mathrm{p}} + b_2 I, \\
y &= [\,1 \quad 0 \quad 0\,][\,V_t \quad Z \quad V_{\mathrm{p}}\,]^{\mathrm{T}}
\end{aligned} \tag{4}$$

where $a_1 = 1/(R_{\mathrm{p}}C_{\mathrm{p}})$, $a_2 = 1/(R_tC_{\mathrm{n}})$, $b_1 = (1/C_{\mathrm{n}}) + (1/C_{\mathrm{p}}) + (R_t/R_{\mathrm{p}}C_{\mathrm{p}})$, $b_2 = 1/C_{\mathrm{p}}$.

This battery model is not linear if V_{oc} is not linearly proportional to the SOC Z. Actually V_{oc} is rather piecewise linear with respect to Z. The relationship is developed from the cell experimental data, where open circuit voltage (OCV) tests are performed on successive discharge of the battery, by the application of periodic current discharge. As for the temperature variation from +55 to −30 °C, the OCV of a lithium-polymer battery (LI-PB) varies non-linearly over the battery SOC as can be seen in Fig. 2.

In order to develop piecewise linear model, define $V_{\mathrm{oc}}(Z) = \kappa Z + d$ for some range of Z and thus κ is not a constant but varies depending on the Z. d_i is defined as V_{oc} linearization error caused by the piecewise linearization

$$\begin{aligned}
\dot{V}_t &= -a_1 V_t + a_1\kappa Z + b_1 I + d_1 = -a_1 V_t + a_{11} Z + b_1 I + d_1, \\
\dot{Z} &= a_2 V_t - a_2\kappa Z - a_2 V_{\mathrm{p}} + d_2 = a_2 V_t - a_{22} Z - a_2 V_{\mathrm{p}} + d_2, \\
\dot{V}_{\mathrm{p}} &= -a_1 V_{\mathrm{p}} + b_2 I + d_3
\end{aligned} \tag{5}$$

This model is not accurate compared with the real cell data. Therefore, the unknown non-linear disturbances terms are added to the model to compensate for the modeling errors

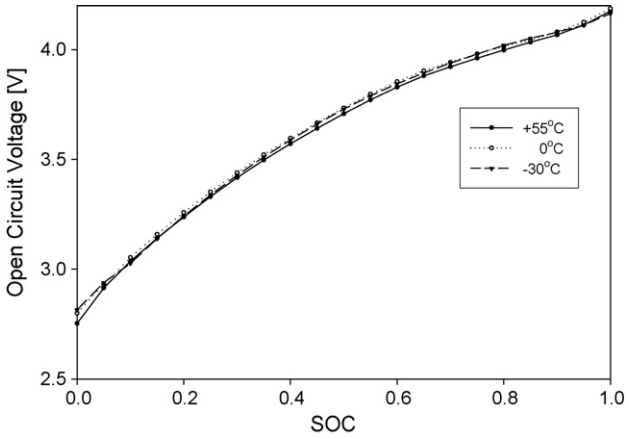

Fig. 2. Open circuit voltage vs. SOC of the lithium-polymer battery.

$$\begin{aligned}
\dot{V}_t &= -a_1 V_t + a_{11} Z + b_1 I + \Delta f_1, \\
\dot{Z} &= a_2 V_t - a_{22} Z - a_2 V_{\mathrm{p}} + \Delta f_2, \\
\dot{V}_{\mathrm{p}} &= -a_1 V_{\mathrm{p}} + b_2 I + \Delta f_3
\end{aligned} \tag{6}$$

where $\Delta f_1, \Delta f_2, \Delta f_3$ not only represent non-linearities caused by linearization error d_i and modeling error, but also time-varying terms and internal/external disturbances. It can be decomposed as

$$\Delta f_1 = \Gamma_1 \xi, \qquad \Delta f_2 = \Gamma_2 \xi, \qquad \Delta f_3 = \Gamma_3 \xi \tag{7}$$

where Γ_1, Γ_2, Γ_3 are known values and ξ represents unknown quantity whose bound is limited.

Observability of the linear system can be obtained from construction of the observability of matrix O_{M}

$$O_{\mathrm{M}} = [\,C \quad CA \quad CA^2\,]^{\mathrm{T}} \tag{8}$$

where $C = [\,1 \quad 0 \quad 0\,]$ and A is the system parameter matrix given in Eq. (6). When expanded, O_{M} is

$$O_{\mathrm{M}} = \begin{bmatrix} 1 & 0 & 0 \\ -a_1 & a_{11} & 0 \\ a_1^2 + a_{11}a_2 & a_2 a_{11} + a_{22}^2 & a_2 a_{22} + a_1 a_2 \end{bmatrix}^{\mathrm{T}} \tag{9}$$

Under every operating condition, the observability matrix is always full rank. Therefore, the suggested modeling is observable and thus possible to estimate the internal state of the battery.

3. Sliding mode observer design

Consider the following time invariant linear system [13]:

$$\dot{x} = Ax + Bu + \Gamma\xi(x, u) \tag{10}$$

$$y = Cx \tag{11}$$

where $x \in R^{n\times 1}$ is the state vector, $A \in R^{n\times n}$, $B \in R^{n\times m}$ is full rank, $u \in R^{m\times 1}$ is the control input, $C \in R^{n\times m}$ such that CB is a non-singular matrix, and $y \in R^{m\times 1}$ is the output, $\Gamma \in R^{m\times 1}$ and $\xi \in R^{m\times 1}$ is the bounded disturbance input, i.e., such that

$\|\xi\| < h$. The controllability matrix (A, B) is completely controllable and (A, C) is completely observable. It is also assumed that the input–output system is minimum phase.

A sliding mode observer for the system Eq. (10) is

$$\dot{\hat{x}} = A\hat{x} + Bu + H(y - \hat{y}) + \rho\Gamma\,\mathrm{sgn}(y - \hat{y}) \tag{12}$$

$$\hat{y} = C\hat{x} \tag{13}$$

where the gain matrix H and the switching gain ρ are chosen so that the stability of the observer system is preserved. The discontinuous feedback input is defined as

$$\mathrm{sgn}(e_y) = \begin{cases} +1, & e_y > 0 \\ -1, & e_y < 0 \end{cases} \tag{14}$$

The state reconstruction error is defined as $e = x - \hat{x}$. Subtracting Eq. (10) from Eq. (12) gives the dynamical reconstruction error system as

$$\begin{aligned} \dot{e} &= Ae - HCe + \Gamma\xi(x, u) - \rho\Gamma\,\mathrm{sgn}(Ce) \\ &= (A - HC)e + \Gamma\xi(x, u) - \rho\Gamma\,\mathrm{sgn}(Ce) \end{aligned} \tag{15}$$

$$e_y = y - \hat{y} = Ce \tag{16}$$

The feedforward gain matrix H can be obtained in two ways; pole assignment method and LQ method. The LQ method is easier to obtain gain matrix H using the Riccati equation as

$$AP + PA^{\mathrm{T}} - PC^{\mathrm{T}}R^{-1}CP = -Q \tag{17}$$

where Q, R are arbitrary semi-positive definite and positive definite matrices, respectively, has a positive definite solution P. Then $A^{\mathrm{T}} - C^{\mathrm{T}}H^{\mathrm{T}}$ is stable with

$$H^{\mathrm{T}} = R^{-1}CP \tag{18}$$

which is equivalent to the stability of $A - HC$. In fact H is the observer gain matrix for the system Eq. (10).

By using appropriate Lyapunov equation we select a matrix W such that the reconstruction error system is asymptotically stable.

Let P_{f} be the positive definite solution of the Lyapunov equation

$$(A - HC)P_{\mathrm{f}} + P_{\mathrm{f}}(A - HC)^{\mathrm{T}} = -Q_{\mathrm{f}} \tag{19}$$

where Q_{f} is an arbitrary positive definite matrix. Set

$$\Gamma^{\mathrm{T}}P_{\mathrm{f}} = WC \tag{20}$$

Then the asymptotically stability of the reconstruction error system is guaranteed if W is a positive definite matrix.

A Lyapunov function candidate for Eq. (15) is

$$V(e) = e^{\mathrm{T}}P_{\mathrm{f}}e \tag{21}$$

Then

$$\begin{aligned} \dot{V}(e) &= \dot{e}^{\mathrm{T}}P_{\mathrm{f}}e + e^{\mathrm{T}}P_{\mathrm{f}}\dot{e} = e^{\mathrm{T}}((A - HC)P_{\mathrm{f}} + P_{\mathrm{f}}(A - HC)^{\mathrm{T}})e \\ &\quad + (\Gamma^{\mathrm{T}}\xi - \rho\Gamma^{\mathrm{T}}\,\mathrm{sgn}(ce))P_{\mathrm{f}}e \\ &\quad + e^{\mathrm{T}}P_{\mathrm{f}}(\Gamma^{\mathrm{T}}\xi - \rho\Gamma^{\mathrm{T}}\,\mathrm{sgn}(ce)) \\ &= -e^{\mathrm{T}}Q_{\mathrm{f}}e + 2(\Gamma^{\mathrm{T}}P_{\mathrm{f}}e\xi - \rho\Gamma^{\mathrm{T}}P_{\mathrm{f}}e\,\mathrm{sgn}(e_y)) \\ &= -e^{\mathrm{T}}Q_{\mathrm{f}}e + 2(WCe\xi - \rho WCe\,\mathrm{sgn}(e_y)) \\ &= -e^{\mathrm{T}}Q_{\mathrm{f}}e + 2W(e_y\xi - \rho e_y\,\mathrm{sgn}(e_y)) \\ &= -e^{\mathrm{T}}Q_{\mathrm{f}}e + 2We_y(\xi - \rho\,\mathrm{sgn}(e_y)) \end{aligned} \tag{22}$$

The $-e^{\mathrm{T}}Q_{\mathrm{f}}e$ is always negative and the latter part of the equation is

$$\begin{aligned} &e_y(\xi - \rho\,\mathrm{sgn}(e_y)) < 0 \quad \text{for } e_y > 0, \text{ if } \rho > h; \\ &e_y(\xi - \rho\,\mathrm{sgn}(e_y)) < 0 \quad \text{for } e_y < 0, \text{ if } \rho > h \end{aligned} \tag{23}$$

where h is a boundary value for ξ.

Then the resultant equation will be

$$\dot{V}(e) < 0 \tag{24}$$

Therefore

$$\lim_{t\to\infty} e(t) = 0 \tag{25}$$

4. Cell parameter extraction

The large size Li-PB was used for the test. The cell comprises of a $LiMn_2O_4$ cathode, an artificial graphite anode and is designed for high power application. It has a nominal capacity of 5.0 Ah and a nominal voltage of 3.8 V. The dimension of the cell is 250 mm × 125 mm × 5 mm and weight of the cell is 120 g. The thermal chamber and the Nittetsu cycler were used as charge–discharge equipments for temperature regulations. Nittetsu cycler has 0–5 V voltage measurement range and 0–120 A current measurement. The cycler's voltage measurement accuracy is ±5 mV and its current measurement accuracy is ±200 mA. It also has precision ampere-hour counter for direct SOC calculation. True SOC was directly obtained from this ampere-hour counter. The test was performed with fully charged condition to set the SOC to one. As test proceeds, the true SOC was calculated by the ampere-hour counter.

Cell characterization tests were performed to extract cell parameters. The parameters are based on the nominal data which is obtained from 25 °C temperature test result. The modeling errors and uncertainties values are obtained from the boundaries of the operating temperature which ranges from −30 to 55 °C. This method can be applied to other kinds of batteries by changing the nominal parameters.

This set of test comprised a sequence of constant current discharges for 180 s and rests for 3600 s. The cell started fully charged up to 4.2 V before the test begins. The discharge current is 5 A and it corresponds to the 1-C rate of the nominal capacity. This amounts to 5% decrease of SOC for each period. The sampled data is collected every second. The purpose of this test is to set the OCV over the entire SOC range and the test result was shown in Fig. 2.

The result comparing the electrical modeling with the cell's test data is shown in Fig. 3. It shows the discharge current, true cell voltage, modeling cell voltage and the modeling voltage

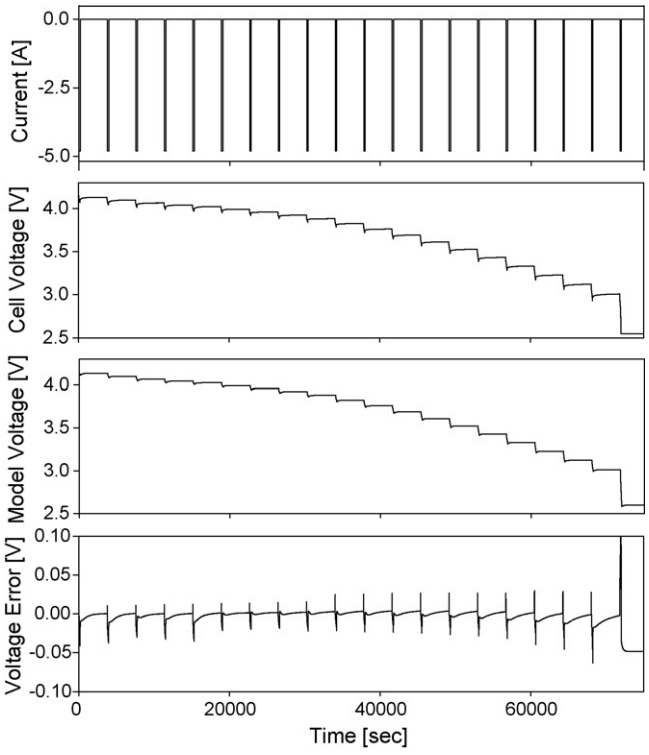

Fig. 3. Current, voltages for true and model cell, and error.

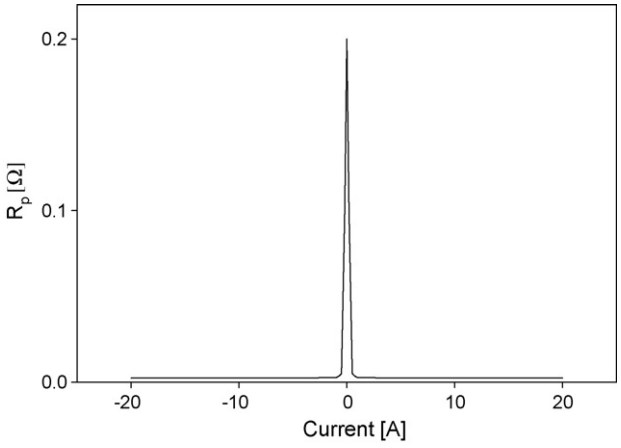

Fig. 4. The polarization resistance R_p.

error. The shapes of the true cell response and the model output are similar in general, although many details of the true cell response are different. This is mainly due to the non-linear characteristics of the nominal capacitance C_n of the true cell and also to the fact that the values of resistances are changed by the SOC. The model parameters are calculated to match with the test data and the resultant values are $C_n = 5$ Ah, $C_p = 200$ F, $R_t = 0.001\ \Omega$, $R_b = 0.003\ \Omega$, and R_p is a non-linear resistance which varies on the current. The plot of R_p over current is shown in Fig. 4.

5. Experimental result for SOC estimation

This data was used to identify nominal parameters for state modeling of the battery. The model parameter are given $a_1 = 1.667$, $a_2 = 0.0589$, $a_{11} = 2.8339$, $a_{22} = 0.1001$, $b_1 = 0.00672$, $b_2 = 0.005$. The uncertainties terms are determined by comparing true cell data with model data to minimize the errors. The system parameters are

$$A = \begin{bmatrix} -1.667 & 2.8339 & 0 \\ 0.0589 & -0.1001 & -0.0589 \\ 0 & 0 & -1.667 \end{bmatrix},$$

$$B = \begin{bmatrix} 0.00672 \\ 0 \\ 0.005 \end{bmatrix}, \qquad \Delta f = \begin{bmatrix} 0.2 \\ 0.2 \\ 1 \end{bmatrix} \xi$$

Assume ξ is a bounded random signal satisfying $\|\xi\| < 0.1$. Choosing $R = 1$, $Q = I_3$, then the positive definite solution of Riccati equation Eq. (17) is

$$P = \begin{bmatrix} 1.3629 & 0.9530 & -0.0046 \\ 0.9530 & 1.0241 & -0.0077 \\ -0.0046 & -0.0077 & 0.2999 \end{bmatrix}$$

From Eq. (18) H is

$$H = \begin{bmatrix} 1.3629 \\ 0.9530 \\ -0.0046 \end{bmatrix}$$

Note that the eigenvalues of $A - HC$ are $-1.5640 \pm 0.6223i$, -1.6689. Let $Q_f = 5I_3$. The positive definite matrix of the Lyapunov equation Eq. (19) is

$$P_f = \begin{bmatrix} 3.0645 & 2.3942 & -0.0179 \\ 2.3942 & 3.6108 & -0.0347 \\ -0.0179 & -0.0347 & 1.4997 \end{bmatrix}$$

Let $W = 1$ and choosing $\rho = 0.2$ as switching gain, then the resultant observer system error reduces to zero by Eq. (24).

The configuration of observer system is shown in Fig. 5. The cell model parameters are obtained by off-line cell test results and the sliding mode observer equations are established by on-line for charge/discharge current of the LI-PB as can be seen in Fig. 5. The charge/discharge current is applied to the LI-PB and sliding mode observer simultaneously. The terminal voltage of the LI-PB is measured as output and fed into the sliding mode observer to compensate for the errors, and output of the observer is the estimated SOC. The controller has been built with infineon 16-bit microprocessor XC167-40 MHz. The calculation time for one cell including current and voltage measurement is around 10 ms. Conventional methods for Kalman filters may take 50 ms for example.

The results of SOC estimation using sliding mode observer are shown in Fig. 6. The estimated model output is controlled with respect to cell terminal voltage with switching ripple, and the estimated SOC follow the true SOC although it has some deviation at the start/end of rest period. This is caused by the discontinuous current and is affected by the abrupt change of R_p. In the discontinuous period, the sliding trajectory is away

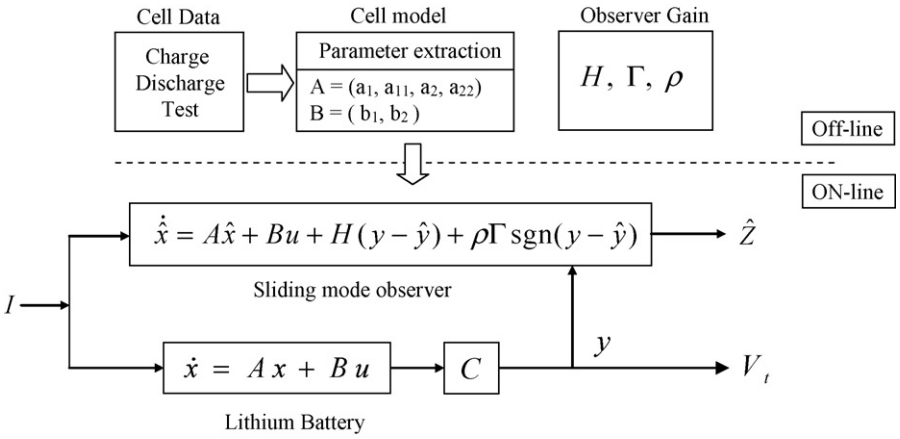

Fig. 5. Configuration of the proposed observer system.

from the sliding surface by the discontinuous function, but the trajectory tracks into the sliding surface in a short time. The one cycle of Fig. 6 is shown in Fig. 7. The estimated output voltage tracks cell voltage with chattering ripples. The estimated SOC also tracks true SOC with chattering ripples. The average value of the estimated SOC is close to the true SOC. This result shows the proposed sliding mode observer can track SOC accurately although the cell modeling is not accurate.

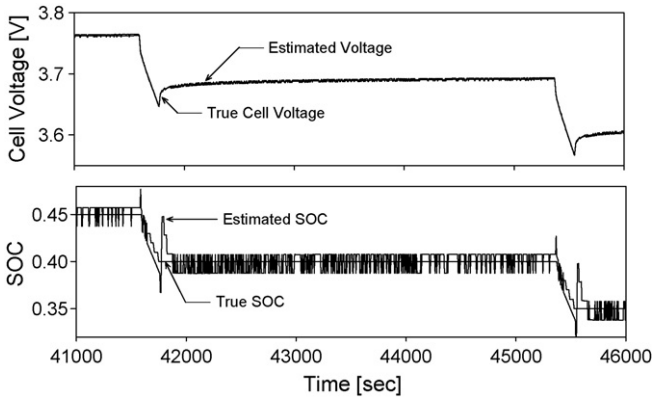

Fig. 7. One cycle plot of Fig. 6.

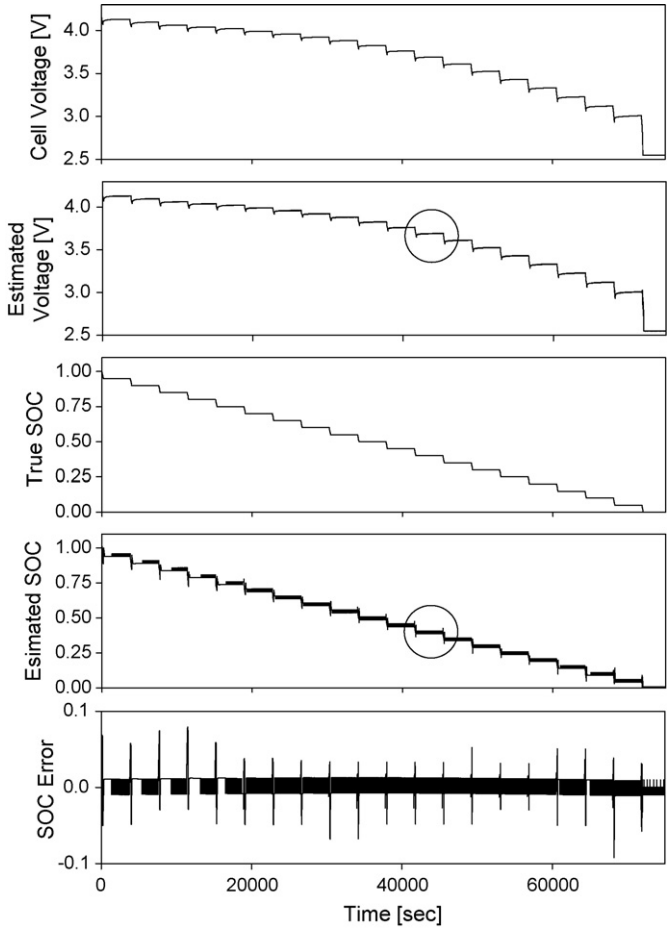

Fig. 6. The results of proposed sliding mode observer.

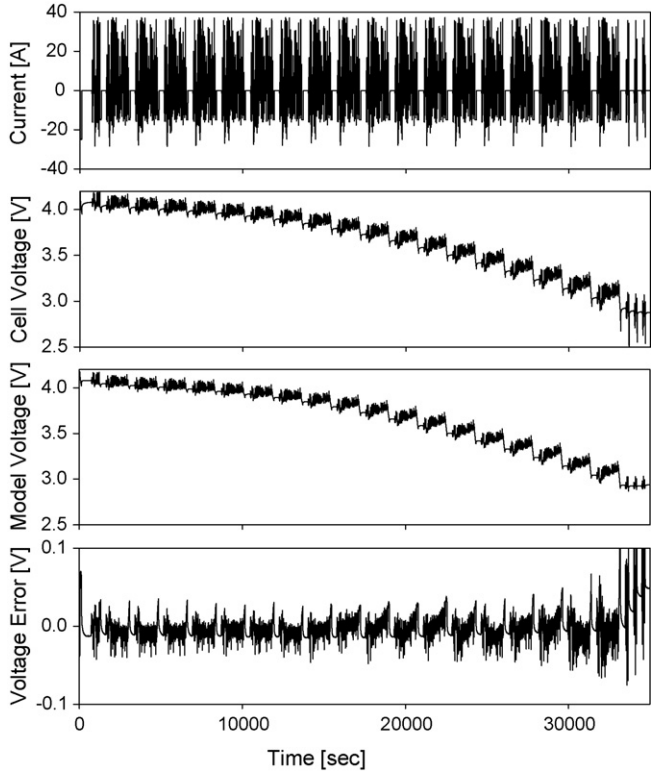

Fig. 8. The results of whole UDDS test.

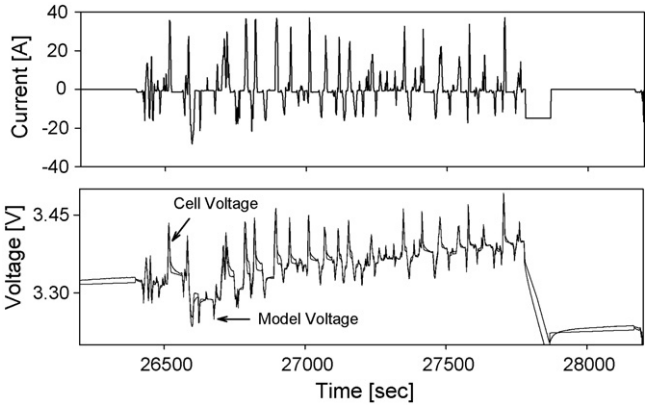

Fig. 9. One UDDS test cycle result for model voltage.

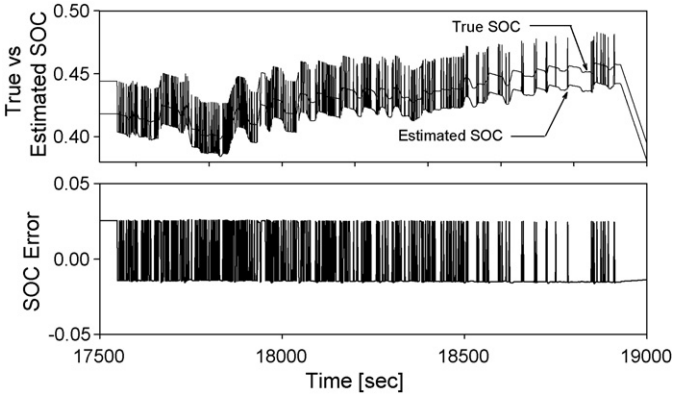

Fig. 11. One cycle result of the estimated SOC and error.

To verify the performance of the proposed observer at the real driving situation, the second test was performed as a sequence of 20 urban dynamometer driving schedule (UDDS) cycles. It is operated by series of charge–discharge pulses and 5 min rests, and spread over the 100–0% SOC range. It can be seen that the SOC decreases by about 5% during each UDDS cycle. Fig. 8 shows the result of overall UDDS cycle current, true cell and model cell voltage, their voltage error. The modeling error is less than 20 mV for 20–80% of SOC range. For clear view, the one cycle of UDDS is shown in Fig. 9. The proposed sliding mode observer was applied to the overall UDDS cycle. The resultant SOC for whole UDDS cycle has been shown in Fig. 10. The estimated SOC and error for whole UDDS cycles are shown in the figure. The SOC error is bounded to 3% of all the cases. The trajectory of the estimated SOC and error for the one UDDS cycle are shown in Fig. 11 in order to show clear view of the sliding mode observer behavior. The trajectories are always confined to the true SOC with the chattering value. This chattering can be smoothed by saturation function instead of sign function. In other way, the average value of the estimated SOC can be close to the true SOC. In this way, the suggested sliding mode observer can be directly applied to the HEV environment with superior performance.

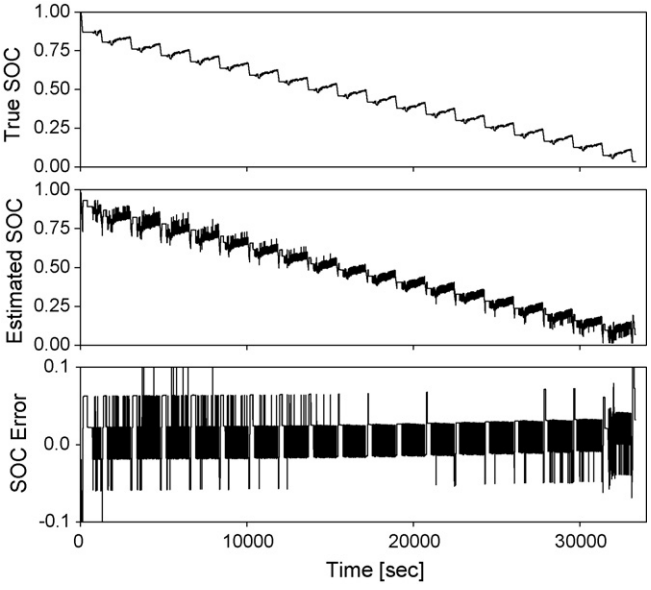

Fig. 10. Estimated SOC and error for UDDS cycles.

6. Conclusions

The sliding mode observer design method for LI-PB state of charge estimation has been presented in this paper. The simple R–C model was used for Li-PB modeling and the modeling errors or uncertainties caused by the simple model were compensated by the proposed sliding mode observer system. The systematic design method has been presented and the Lyapunov inequality equation has proved convergence of the proposed observer. The performance of the proposed system has been verified by the UDDS cycle test which is very harsh environmental test. The SOC error is confined to the acceptable level, less than 3% in most cases which is applicable to the real environments.

References

[1] O. Caumont, Ph. Le Moigne, P. Lenain, C. Rombaut, Electric Vehicle Symposium, vol. EVS-15, Brussels, Belgium, 1998, pp. 30–33.
[2] S. Rodrigues, N. Munichandraiah, A.K. Shukla, J. Power Source 87 (2000) 12–20.
[3] B.S. Bhangu, P. Bentley, D.A. Stone, C.M. Bingham, IEEE Trans. Vehicular Technol. 54 (3) (2005) 783–794.
[4] G.L. Plette, J. Power Source 134 (2004) 262–276.
[5] C.C. Chan, E.W.C. Lo, S. Weixiang, J. Power Source 87 (2000) 201–204.
[6] P. Singh, C. Fennie, D.E. Reisner, A. Salkind, in: Electric Vehicle Symposium, vol. EVS-15, Brussels, Belgium, September 30–33, 1998 Proceedings on CD-ROM.
[7] V.I. Utkin, Sliding Modes and their Applications in Variable Structure Systems, MIR, Moscow, Russia, 1978.
[8] I. Haskara, U. Ozguner, V. I. Utkin, IEEE Workshop on Variable Structure System, 1996, pp. 193–198.
[9] Y. Xiong, M. Saif, Proceedings of the 39th IEEE conference on Decision and Control, 2000, pp. 316–327.
[10] H. Ramirez, R. Ortega, R. Moreno, M. Esteban, Proceedings of the 34th Conference on Decision and Control, 1995, pp. 3379–3383.
[11] M. Doyle, T.T. Fuller, J. Newman, J. Electrochem. Soc. 140 (1993) 1526.
[12] S. Pang, J. Farrell, J. Du, M. Barth, Proceeding of the American Control Conference, 2001, pp. 1644–1649.
[13] A. Jafari Koshkouei, A.S.I. Zinober, Proceedings of the 34th Conference on Decision & Control, 1995, pp. 2115–2120.